

# Statistical Properties of Eigenstates in three-dimensional Mesoscopic Systems with Off-diagonal or Diagonal Disorder

Branislav K. Nikolic<sup>†</sup>

*Department of Physics and Astronomy, SUNY at Stony Brook, Stony Brook, New York 11794-3800*

The statistics of eigenfunction amplitudes are studied for mesoscopic disordered electronic systems of finite size. The eigenspectrum and eigenstates are obtained by solving numerically the nearest neighbor tight-binding Hamiltonian in three dimensions. Disorder is introduced either in the potential on-site energy (“diagonal”) or in the hopping (“off-diagonal”) between single s-orbitals residing on each site. The samples are characterized by the exact zero-temperature conductance computed using real-space Green function technique and related Landauer-type formula. The comparison of eigenstate statistics in two models of disorder shows sample-specific details which are not fully taken into account by the value of the conductance, shape of the sample and dimensionality. The distribution functions are also contrasted with the universal predictions of Random Matrix Theory valid in the infinite conductance limit.

PACS numbers: 72.15.Rn, 73.23.-b, 05.40.-a

The disorder induced localization-delocalization (LD) transition in solids has been one of the most vigorously pursued problems in condensed matter physics since the seminal work of Anderson.<sup>1</sup> In the thermodynamic limit, strong enough disorder generates zero-temperature critical point in  $d > 2$  dimensions,<sup>2</sup> as a result of quantum interference effects. This has directed research in the “pre-mesoscopic” era<sup>3</sup> toward the viewpoint provided by the theory of critical phenomena.<sup>4</sup> The advent of mesoscopic quantum physics<sup>5</sup> has unearthed large fluctuations, induced by quantum coherence and randomness of disorder,<sup>6</sup> of various physical quantities<sup>7</sup> (e.g., conductance, local density of states, current relaxation times, etc.), even well into the delocalized phase. Thus, complete understanding of the LD transition requires to examine the full distribution functions of relevant quantities.<sup>8</sup> Especially interesting are their deviations, caused by the incipient localization, from the (usually) Gaussian distribution expected in the limit of infinite dimensionless conductance  $g = G/G_Q$  (in units of the conductance quantum  $G_Q = 2e^2/h$ ). This paper presents the study of such type—numerical computation of the statistics of eigenfunction amplitudes in a finite-size three-dimensional (3D) nanoscale (composed of  $\sim 1000$  atoms) mesoscopic disordered conductors. Such conductors are often “neglected” in favor of the more popular playgrounds—two-dimensional systems (2D), where one can study states resembling 3D critical wave functions in a wide range of systems sizes and disorder strengths,<sup>9</sup> or quasi one-dimensional systems<sup>10</sup> where analytical techniques can handle even non-perturbative phenomena (at small  $g$ ).<sup>11,12</sup> In 3D systems critical (i.e., multifractal) eigenfunctions appear only at the mobility edge  $E_c$ , which separates extended and localized states inside the energy band.

The physics of disordered conductors is captured by studying the quantum dynamics of a non-interacting (quasi)particle in a random and confining potential. This problem is classically non-integrable, thereby exhibiting

quantum chaos. The concepts unifying disordered electron physics and standard examples of quantum chaos<sup>13</sup> come from the statistical approach to the properties of energy spectrum and corresponding eigenstates, which can not be computed analytically. While energy level statistics of disordered systems have been explored to a great extent,<sup>14,15</sup> the investigation of statistical properties of eigenfunctions and their relation to quantum transport has been initiated only recently.<sup>16</sup> Such studies are not only divulging peculiar spectral properties of random Hamiltonians, but are relevant for the thorough understanding of various unusual transport properties of diffusive metallic samples. The standard examples are long-time tails in the relaxation of current<sup>17</sup> or log-normal tails (in  $d = 2 + \epsilon$ ) of the distribution function of mesoscopic conductances.<sup>7</sup> Also, tunneling experiments on quantum dots probe the coupling to external leads, which depends sensitively on the local features of wave functions.<sup>18</sup> Experiments which are the closest to directly delving into the microscopic structure of quantum chaotic or disordered wave functions exploit the correspondence between the Schrödinger and Maxwell equations in microwave cavities.<sup>19</sup>

The study of fluctuations and correlations of eigenfunction amplitudes<sup>16,20</sup> in mesoscopic systems has lead to the concept of the so-called pre-localized states.<sup>17,21</sup> This notion refers to anomalously rare states which have sharp amplitude peaks on the top of an extended background (in the 3D delocalized phase) even though the disordered sample can be in the diffusive,  $\ell \ll L < \xi$ , metallic ( $g \gg 1$ ) regime. Here  $\ell$  is the elastic mean free path and  $\xi$  is the localization length (which plays the role of a phase transition correlation length<sup>6</sup>  $\xi_c$  in  $d \leq 2$ ). Therefore, pre-localized states are putative precursors of LD transition, and they determine the asymptotic tails of various distribution functions. In  $d \leq 2$ , where all states are considered to be localized,<sup>4</sup> pre-localized states have anomalously short localization radius<sup>16</sup> when compared to “ordinary” localized states in low-dimensional

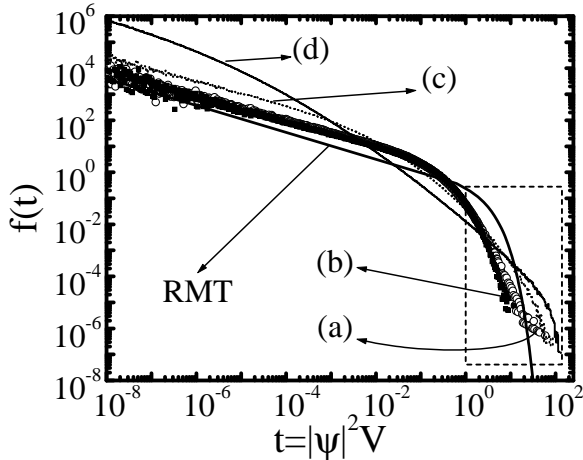


FIG. 1. Statistics of wave function intensities in the RH Anderson model, with  $W_{\text{RH}} = 1$ , on a simple cubic lattice with  $N = 16^3$  sites. The distribution function  $f(t)$ , Eq. (1), is computed for the states around the following energies: (a)  $E = 0$ , (b)  $E = 1.5$ , (c)  $E = 2.55$ , and (d)  $E = 2.75$ . Disorder averaging is performed over  $N_{\text{Ens}} = 40$  different samples. The Porter-Thomas distribution (3) is denoted by RMT. The part of the distributions inside the dashed box is enlarged on Fig. 2.

systems. They are responsible<sup>21</sup> for multifractal scaling (which stem from  $L < \xi = \xi_c$ ) in weakly localized ( $g \gg 1$ ) 2D conductors. In 3D the correlation length is always microscopic ( $\sim \lambda_F$ ) for good metallic samples, and no multifractal states are expected.<sup>6</sup> The appearance of small regions inside disordered solids where eigenstates can have large amplitudes seems to be a “strongly pronounced” analog<sup>9,19</sup> of the phenomenon of scarring<sup>22</sup> (anomalous enhancement or suppression of quantum chaotic wave function intensity on the unstable periodic orbits in the corresponding classical system).

In general, the study of properties of wave functions on a scale smaller than  $\xi$  should probe quantum effects causing evolution of extended into localized states upon approaching the LD critical point. In the marginal two-dimensional case, the divergent (in the limit  $L \rightarrow \infty$ ) weak localization (WL) correction<sup>23</sup> to the semiclassical Boltzmann conductivity provides an explanation of localization in terms of the interference between two amplitudes to return to initial point along the same classical path in the opposite directions.<sup>24</sup> This then leads to a coherent backscattering (i.e., suppression of conductivity) in a time-reversal invariant systems without spin-orbit interaction. However, in 3D systems WL correction is not “strong” enough to provide a full microscopic picture of quantum interference effects responsible for LD transition, and thus facilitate the development of “quantum intuition”.

Here I expose the results for the statistics of eigenfunction “intensities”  $|\psi_\alpha(\mathbf{r})|^2$  in 3D (closed) mesoscopic conductors characterized by two different types of micro-

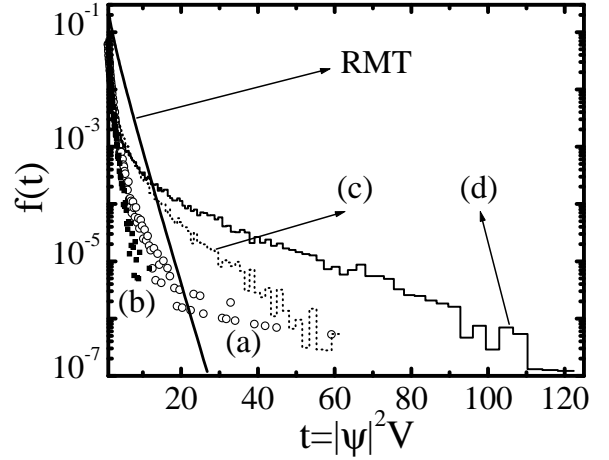


FIG. 2. Statistics of wave function intensities in the RH Anderson model, with  $W_{\text{RH}} = 1$ , on a simple cubic lattice with  $N = 16^3$  sites. This Figure plots the same distributions  $f(t)$  as the ones plotted on Fig. 1, in the range defined by the dashed square on Fig. 1. The same labels apply to both Figures.

scopic disorder. Numerical methods employed make it possible to treat both perturbative and non-perturbative phenomena as well as the crossover realm in between. The statistical properties of eigenstates are embodied in the disorder-averaged distribution function<sup>9,21</sup>

$$f(t) = \frac{1}{\rho(E)N} \left\langle \sum_{\mathbf{r},\alpha} \delta(t - |\Psi_\alpha(\mathbf{r})|^2 V) \delta(E - E_\alpha) \right\rangle, \quad (1)$$

on  $N$  discrete points  $\mathbf{r}$  inside a sample of volume  $V$ . Here  $\rho(E) = \sum_\alpha \delta(E - E_\alpha)$  is the mean level density at energy  $E$ . Averaging over disorder is denoted by  $\langle \dots \rangle$ . Normalization of eigenstates gives  $\langle t \rangle = \int dt t f(t) = 1$ . A finite-size disordered sample is modeled by a tight-binding Hamiltonian (TBH) with nearest neighbor hopping  $t_{\mathbf{mn}}$

$$\hat{H} = \sum_{\mathbf{m}} \varepsilon_{\mathbf{m}} |\mathbf{m}\rangle \langle \mathbf{m}| + \sum_{\langle \mathbf{m}, \mathbf{n} \rangle} t_{\mathbf{mn}} |\mathbf{m}\rangle \langle \mathbf{n}|, \quad (2)$$

on a simple cubic lattice  $16 \times 16 \times 16$ . Each site  $\mathbf{m}$  contains a single orbital  $\langle \mathbf{r} | \mathbf{m} \rangle = \psi(\mathbf{r} - \mathbf{m})$ . Periodic boundary conditions are chosen in all directions. In the random hopping (RH) model the disorder is introduced by taking the off-diagonal matrix elements to be a uniformly distributed random variable,  $1 - 2W_{\text{RH}} < t_{\mathbf{mn}} < 1$  (diagonal elements are zero,  $\varepsilon_{\mathbf{m}} = 0$ ). The strength of the disorder is measured by  $W_{\text{RH}}$ . The other model studied here is the standard diagonally disordered (DD) Anderson model with potential energy  $\varepsilon_{\mathbf{m}}$  on site  $\mathbf{m}$  drawn from the uniform distribution,  $-W_{\text{DD}}/2 < \varepsilon_{\mathbf{m}} < W_{\text{DD}}/2$ , and  $t_{\mathbf{mn}} = 1$  as the unit of energy. The Hamiltonian (2) is a real symmetric matrix because time-reversal symmetry is assumed. The results for  $f(t)$  in the samples described by

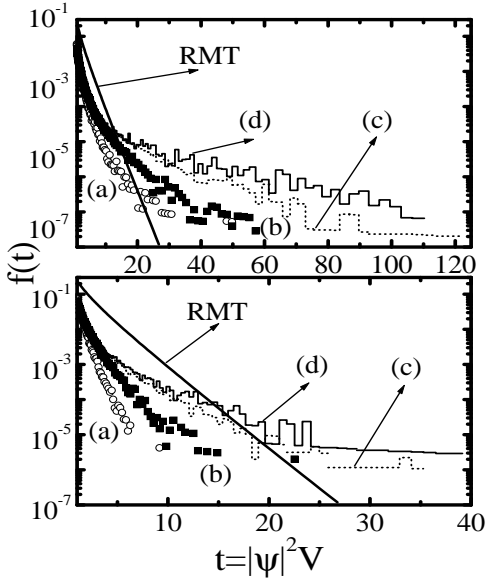


FIG. 3. Statistics of wave function intensities in the DD Anderson model on a simple cubic lattice with  $N = 16^3$  sites. The distribution function  $f(t)$ , Eq. (1), is computed for the states around following energies. Upper panel,  $W_{\text{DD}} = 10$ : (a)  $E = 0$ , (b)  $E = 6.0$ , (c)  $E = 7.45$ , and (d)  $E = 7.85$ . Lower panel,  $W_{\text{DD}} = 6$ : (a)  $E = 0$ , (b)  $E = 4.1$ , (c)  $E = 6.56$ , and (d)  $E = 6.7$ . Disorder averaging is performed over  $N_{\text{Ens}} = 40$  different samples. The Porter-Thomas distribution (3) is denoted by RMT.

the RH and DD Anderson models are shown on Figs. 1, 2 and Fig. 3, respectively. Although some of the samples are characterized by similar values of conductance, the eigenstates in the two models show different statistical behavior. In what follows the meaning of these findings is explained in the context of statistical approach to quantum systems with non-integrable classical dynamics. In particular, the results are compared to the universal predictions of Random Matrix Theory (RMT).

In the statistical approach<sup>15</sup> of RMT the (random) Hamiltonian of a quantum chaotic system is replaced<sup>25</sup> by a random matrix drawn from an ensemble defined by the symmetries under time-reversal and spin-rotation. This leads to the Wigner-Dyson (WD) statistics for eigenvalues and Porter-Thomas (PT) distribution for eigenfunction intensities. For the Gaussian Orthogonal Ensemble (GOE), relevant for studies of time-reversal-invariant Hamiltonians like (2), the PT distribution is given by

$$f_{\text{PT}}^0(t) = \frac{1}{\sqrt{2\pi t}} \exp(-t/2). \quad (3)$$

The function  $f_{\text{PT}}^0(t)$  is plotted as a reference on Figs. 1, 2 and Fig. 3. The predictions of RMT are universal, depending only on the symmetry properties of the relevant ensemble. They apply to the statistics of real disordered systems<sup>27</sup> in the limit  $g \rightarrow \infty$  ( $g = E_{\text{Th}}/\Delta$ ,

where  $\Delta = 1/\rho(E)$  is the mean energy level spacing and  $E_{\text{Th}} = \hbar D/L^2$  is the Thouless energy, set by the classical diffusion with diffusion constant  $D$ ). The spectral correlations in RMT are determined by logarithmic level repulsion which is independent of true dynamics. All sample-specific details are absorbed into the mean level spacing  $\Delta$ . Also, the level correlations are independent of the eigenstate correlations. The RMT answer (3) for the distribution function (1) was derived by Porter and Thomas<sup>28</sup> by assuming that the coordinate-representation eigenstate  $\langle \mathbf{r} | \psi_\alpha \rangle$  in a disordered (or classically chaotic system) is a Gaussian random variable. This simple behavior occurs only in systems with unbroken or completely broken time-reversal symmetry.<sup>29</sup> Thus, RMT implies the statistical equivalence of eigenstates. They equally test the random potential all over the sample, and typical wave function has uniform amplitude up to inevitable Gaussian fluctuations.

Microscopic theory brings corrections to the RMT results in the case of samples with finite  $g$ . In a finite-size sample level statistics follow RMT predictions in the ergodic regime, i.e., on the energy separation scale smaller than  $E_{\text{Th}}$ . Non-universal corrections to the spectral statistics<sup>30</sup> or eigenfunction statistics<sup>31</sup> (which describe the long-range correlations of wave functions) depend on dimensionality, shape of the sample, and conductance  $g$ . These deviations from RMT predictions grow with increasing disorder (i.e., lowering of  $g$ ). At the LD transition wave functions acquire multifractal properties, while the critical level statistics become scale-independent.<sup>32</sup> For strong disorder or, at fixed disorder, for energies  $|E|$  above the mobility edge  $|E_c|$ , wave functions are exponentially localized. A typical wave function decays as  $\psi(r) = p(r) \exp(-r/\xi)$  from its maximum centered at an arbitrary point inside the sample of size  $L > \xi$ . Here  $p(r)$  is a random function and approximately radial symmetry of decay is assumed. Since two states close in energy are localized at different points in space, there is almost no overlap between them. Therefore, the levels become uncorrelated and obey Poisson statistics. If  $p(r) = c$  is simplified to a normalization constant the distribution function of intensities is given by<sup>9</sup>

$$f_\xi(t) = \frac{\pi \xi^2 \ln(c^2 V/t)}{2V} \frac{1}{t}, \quad (4a)$$

$$c^2 = \frac{2}{\pi \xi^2} \left( 1 - \left( 1 + \frac{L}{\xi} \right) \exp(-L/\xi) \right)^{-1}, \quad (4b)$$

where a radially symmetric sample (radius  $L/2$ ) is assumed.

The distribution function  $f(t)$  is equivalently given in term of its moments  $b_q = \int dt t^q f(t)$ . For the orthogonal ensemble the PT distribution (3) has moments  $b_q^{\text{PT}} = 2^q V^{-q+1} \Gamma(q+1/2)/\Gamma(1/2)$ . They are related to the moments  $I_\alpha(q) = \int d\mathbf{r} |\psi_\alpha(\mathbf{r})|^{2q}$  of the wave function intensity  $|\psi_\alpha(\mathbf{r})|^2$ . In the finite  $g$  case the spatial correlations of wave function amplitudes at distances comparable to the system size are non-negligible. Therefore

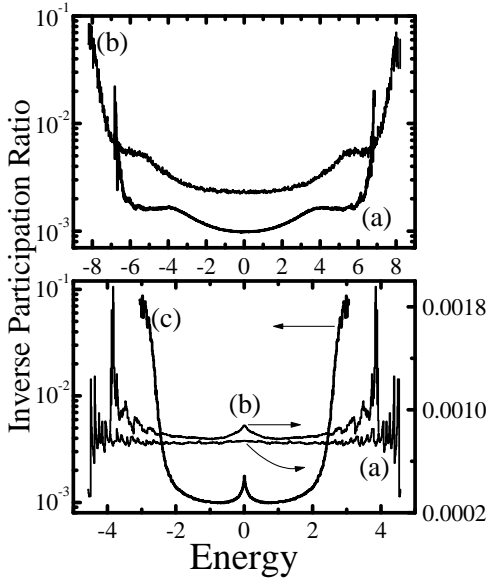


FIG. 4. Inverse Participation Ratio  $\bar{I}(2)$ , averaged over both 40 different conductors and small energy bins, of eigenstates in the RH and DD Anderson models on a simple cubic lattice with  $N = 16^3$  sites. Top: diagonal disorder with (a)  $W_{DD} = 6$ , and (b)  $W_{DD} = 10$ . Bottom: off-diagonal disorder with (a)  $W_{RH} = 0.25$ , (b)  $W_{RH} = 0.375$ , and (c)  $W_{RH} = 1$ .

$I_\alpha(q)$  fluctuates from state to state and from sample to sample.<sup>16</sup> In the universal regime  $g \rightarrow \infty$  wave functions cover the whole volume with only short-range correlations (on the scale  $|\mathbf{r}_1 - \mathbf{r}_2| \lesssim \ell$ ) persisting between  $\Psi_\alpha(\mathbf{r}_1)$  and  $\Psi_\alpha(\mathbf{r}_2)$ . This means that integration in the definition of  $I_\alpha(q)$  provides self-averaging and  $I_\alpha(q)$  does not fluctuate in the universal limit, i.e.,  $I_\alpha(q) = b_q^{\text{PT}}$ . Following Wegner,<sup>33</sup> individual states, in the analysis to follow, are characterized by an ensemble average of  $I_\alpha(q)$

$$\bar{I}(q) = \Delta \left\langle \sum_{\mathbf{r}, \alpha} |\Psi_\alpha(\mathbf{r})|^{2q} \delta(E - E_\alpha) \right\rangle. \quad (5)$$

The moment  $I_\alpha(2)$  is usually called inverse participation ratio (IPR). It is a one-number measure of the degree of localization (i.e., it measures the portion of space where the amplitude of the wave function differs markedly from zero). This is seen from the scaling properties of moments  $\bar{I}(q)$  with respect to system size

$$\bar{I}(q) \propto \begin{cases} L^{-d(q-1)} & \text{metal,} \\ L^0 & \text{insulator,} \\ L^{-d^*(q)(q-1)} & \text{critical.} \end{cases} \quad (6)$$

Here  $d^*(q) < d$  is the fractal dimension. Its dependence on  $q$  is the hallmark of multifractality wave functions. These functions are delocalized, but extremely inhomogeneous occupying only an infinitesimal fraction of the sample volume in the thermodynamic limit. The IPR is affected by mesoscopic fluctuations which scale in metallic samples as<sup>20</sup> as  $\delta I_\alpha(2) \sim 1/g^2 \propto L^{4-2d}$ . In the critical

region ( $g \sim 1$ ) fluctuations<sup>20</sup> are of the same order as the average value, which is then not enough to characterize the critical eigenstates (their IPR is not self-averaging<sup>34</sup> even though multifractal wave function extend through the whole sample).

I use  $\bar{I}(2)$  (Fig. 4) as a rough guide in selecting eigenstates with different properties (especially in the delocalized phase). The second parameter used in the “selection procedure” is the conductance  $g(E_F)$  (see below, Fig. 5) computed for the band filled up to the Fermi energy  $E_F$  equal to the state eigenenergy. The conductance as a function of band filling allows us to delineate delocalized from localized phase as well as to narrow down the critical region around LD transition point (which is defined by  $E_c$  when disorder strengths  $W_{RH}$  or  $W_{DD}$  are fixed). Once the potentially interesting states are chosen, their statistical properties are explored in detail by computing  $f(t)$ .

The average IPR for both RH and DD Anderson model is shown on Fig. 4. The models with random hopping<sup>35</sup> have attracted recently considerable attention inasmuch as they show a disorder induced quantum critical point in less than three dimensions,<sup>36,37</sup> where delocalization occurs in the band center ( $E = 0$ ). The real system which correspond to TBH (2) with off-diagonal disorder include doped semiconductors,<sup>35</sup> such as P-doped Si, where hopping matrix elements  $t_{mn}$  vary exponentially with the distances between the orbitals they connect, while diagonal on-site energies  $\varepsilon_m$  are nearly constant. The behavior of low-dimensional RH Anderson model goes against the standard mantra of the scaling theory of localization<sup>4</sup> that all states in  $d \leq 2$  are localized. This is actually known since the work of Dyson<sup>38</sup> on glasses. Also, the scaling theory for quantum wires with off-diagonal disorder requires two parameters<sup>39</sup> which depend on the microscopic model, thus breaking the celebrated universality in disordered electronic problem. In 3D case explored here, the states in the band center are less extended than other delocalized states inside the band (Fig. 4). The off-diagonal disorder is not strong enough<sup>40</sup> to localize all states in the band, in contrast to the usual case of diagonal disorder where whole band becomes localized<sup>41</sup> for  $W_{DD}^c > 16.5$ .

The mobility edge for the strongest RH disorder  $W_{RH} = 1$ , as well as for DD models, is found by looking at an exact zero-temperature static conductance. This quantity (which is a Fermi surface property) is computed from the Landauer-type formula<sup>42</sup> (the factor of two here and in the density of states (8) is for spin degeneracy)

$$G(E_F) = \frac{2e^2}{h} \text{Tr}(\mathbf{t}(E_F)\mathbf{t}^\dagger(E_F)), \quad (7)$$

where transmission matrix  $\mathbf{t}(E_F)$  is expressed in terms of the real-space (lattice) Green functions<sup>43,44</sup> for the sample attached to two ideal (disorder-free) semi-infinite leads. To study the conductance in the whole band of the DD model  $t_{mn} = 1.5$  is used<sup>44</sup> for the hopping parameter

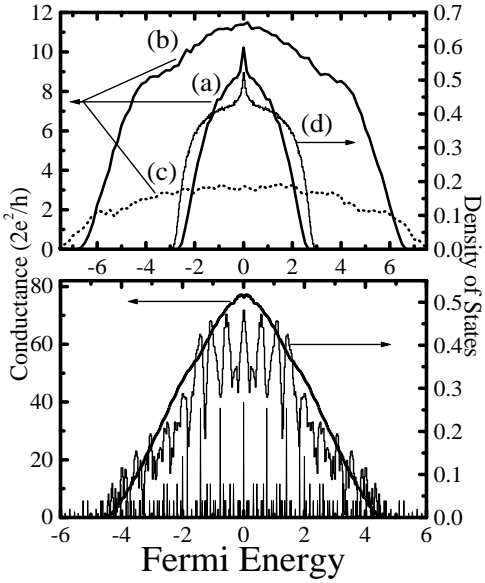


FIG. 5. Conductance and density of states in the RH and DD Anderson models on a simple cubic lattice with  $N = 16^3$  sites. Top: RH disorder, (a) and (d), of strength  $W_{\text{RH}} = 1$  (mobility edge is at  $|E_c| \simeq 2.53$ ); diagonal disorder of strength (b)  $W_{\text{DD}} = 6$  ( $|E_c| \simeq 6.5$ ), and (c)  $W_{\text{DD}} = 10$  ( $|E_c| \simeq 7.4$ ). Disorder averaging is performed over  $N_{\text{Ens}} = 20$  different samples for conductance and  $N_{\text{Ens}} = 40$  for DoS. Bottom: RH disorder  $W_{\text{RH}} = 0.25$ ; sharp lines correspond to the DoS of a clean system on the same lattice (scaled by 1/10 for clarity).

in the leads. This mesoscopic computational technique for transport coefficients “opens” the sample, thereby smearing the discrete levels of initially isolated system. Therefore, the spectrum of *sample+leads=infinite system* becomes continuous and conductance can be calculated at any  $E_F$  inside the band. However, the computed conductance, for not too small disorder or coupling to the leads (of the same transverse width as the sample)<sup>45,46</sup> is practically equal to the “intrinsic” conductance  $g = E_{\text{Th}}/\Delta$  expressed in terms of spectral properties of a closed sample.

The conductance and density of states (DoS)

$$N(E) = 2 \frac{\rho(E)}{V}, \quad (8)$$

are plotted on Fig. 5. The DoS is obtained from the histogram of the number of eigenstates which fall into equally spaced energy bins along the band. The conductance and DoS of the RH model have a peak at  $E = 0$ , which becomes a logarithmic singularity in the limit of infinite system size.<sup>38</sup> For weak off-diagonal disorder ( $W_{\text{RH}} = 0.25$ ),  $N(E)$  still resembles the DoS of a clean system even after ensemble averaging (lower panel of Fig. 5). On the other hand, the conductance is a smooth function of energy since the discrete levels of an isolated sample are broadened by the coupling to leads. The same is true for the DoS computed from the imagi-

nary part of the Green function of an open system. The mobility edge is absent for low RH disorder ( $W_{\text{RH}} = 0.25$  and  $W_{\text{RH}} = 0.375$ ) in systems of the size  $L \leq 16a$ , i.e., localization length  $\xi$  is greater than  $16a$  (lattice spacings is denoted by  $a$ ) for all energies inside the band. For other samples on Fig. 5 the mobility edge appears inside the band. This is clearly shown for  $W_{\text{RH}} = 1$  case where band edge  $E_b$  ( $N(E_b) = 0$ ) differs from  $E_c$ . The mobility edge is located at the minimum energy  $|E_c|$  for which  $\rho(E_c)$  is still different from zero. The conductance of finite samples is always finite, although exponentially small at  $|E_F| > |E_c|$ . The approximate values of  $|E_c|$  listed on Fig. 5 are such that conductance satisfies:  $\rho(E_F) < 0.1$ , for  $|E_F| > |E_c|$ ; typically  $\rho(E_c) \in (0.2, 0.5)$  as in recent detailed studies<sup>47</sup> of conductance properties at  $E_c$ . Thus found  $E_c$  is virtually equal to the true mobility edge, which is defined only in the thermodynamic limit (and is usually obtained from some numerical finite-size scaling procedure<sup>2</sup>). Namely, the position of mobility edge, extracted from the vanishing of conductance of a finite-size sample, will not change<sup>48</sup> when going to larger system sizes if  $\xi < L$  for all energies  $|E| > |E_c|$ .

The distribution  $f(t)$  of eigenfunction intensities has been studied analytically for diffusive conductors close to the universal limit (i.e., conductance is large and localization effects are small) in Refs. 16,21 using the supermatrix  $\sigma$ -model,<sup>11</sup> or by means of a direct optimal fluctuations method.<sup>49</sup> Numerical studies<sup>9</sup> were conducted in 2D for all disorder strengths. Here I study how  $f(t)$  evolves in 3D disordered samples, where a genuine LD transition occurs (either at fixed energy, upon increasing disorder, or vice versa). The complete eigenproblem of a single particle disordered Hamiltonian is solved numerically and  $f(t)$  is computed for the chosen eigenstates in the metallic phase ( $|E| < |E_c|$ ), insulating phase ( $|E| > |E_c|$ ) and close to the mobility edge  $|E_c|$ . The two delta functions in Eq. (1) are approximated by a box function  $\bar{\delta}(x)$ . The width of  $\bar{\delta}(E - E_\alpha)$  is small enough at a specific energy (in a given sample) that  $\rho(E)$  is constant inside that interval. In practice 5–10 states are found in the energy bin, which effectively provides additional averaging over the disorder (according to ergodicity<sup>12,15</sup> in RMT). The width of a broadened delta function of  $t$  is constant on a logarithmic scale. Averaging over the impurity ensemble is performed in order to improve the statistics.<sup>9</sup> The function  $f(t)$  is computed at all points inside the sample, i.e.,  $N = 16^3$  in Eq. (1).

The evolution of  $f(t)$ , when sweeping the band through the “interesting” states, is shown on Figs. 1, 2 for the RH disordered sample. Since pre-localized states are identified through slow decay at high wave function intensities,<sup>11</sup> this region is enlarged on Fig. 2. The same is trivially true for the localized states which exhibit extremely long tails, Eq. (4). Thus, the deviation of  $f(t)$  for pre-localized states from the PT distribution is mostly pronounced in the tails. Such long tails have been observed in distribution functions of other mesoscopic quantities,<sup>6,7</sup> and are signaling the onset of localization. More-

over, all states analyzed here deviate from  $f_{\text{PT}}^0(t)$  in their characteristic way. It is interesting that states in the band center of the RH model, which are responsible for the largest zero-temperature conductance ( $g = 10.2$ ,  $\text{Var } g = 0.63$ ), are in fact pre-localized according to the criterion accepted above.<sup>50</sup> This result, together with the DoS and conductance from Fig. 5, shows that phenomena in the band center of 3D conductors with off-diagonal disorder (whose Hamiltonians have sublattice, or chiral,<sup>35,51</sup> symmetry leading to an eigenspectrum which for  $E_n$  contains  $-E_n$  as well, Fig. 4), are as intriguing as their much studied counterparts in low-dimensional systems.<sup>36,37</sup> In the RH case with  $W_{\text{RH}} = 0.25$  or  $W_{\text{RH}} = 0.375$  all states are extended. Their  $f(t)$  overlaps with the distribution function for the totally delocalized states at  $E = 1.5$  in the sample characterized by  $W_{\text{RH}} = 1$ . The distribution function  $f_\xi(t)$  in Eq. (4), obtained from the simple parameterization of a localized state, does not fit precisely the numerical result for the states corresponding to  $E = 2.75$ . An estimate of the localization length,  $\xi \simeq 5.5a$ , would generate a distribution with a similar tail to that of the analyzed states.

The same statistical analysis is performed for the eigenstates of DD Anderson model (which has been studied extensively throughout the history of localization theory<sup>2,41,53</sup>). Fig. 3 plots different evolutions of  $f(t)$  when changing the maximum of the conductance  $G(E_F)$  (controlled by  $W_{\text{DD}}$ ). The conductance of TBH with  $W_{\text{DD}} = 6$  is numerically close to the conductance of RH disordered samples with  $W_{\text{RH}} = 1$ . Nevertheless, comparison of the corresponding distribution functions reveals model dependent features<sup>16</sup> which are beyond corrections accounted by the eigenmodes of a classical diffusion operator<sup>31,52</sup> (the spectrum of  $\mathcal{D}\nabla^2$ , with appropriate boundary conditions, depends on  $g$ , shape of the sample and dimensionality). For strong DD ( $W_{\text{DD}} = 10$ ) the conductance  $g(E_F)$  is smaller than 3.5. In this regime transport becomes “intrinsically diffusive”,<sup>53</sup> but one can still extract resistivity from the approximate Ohmic scaling of disorder-averaged resistance<sup>53</sup> (for those fillings where<sup>54</sup>  $g(E_F) > 2$ ). However, the close proximity to the critical region  $g \sim 1$  generates long tails of  $f(t)$  (a signature of pre-localization, as discussed above) for all states inside the band. This gives insight in the microscopic structure of eigenstates which carry the current in a non-perturbative transport regime,<sup>11,55</sup> which is characterized by the lack of semiclassical concepts, like mean free path  $\ell$  (unwarranted use of Boltzmann theory in such regime would give<sup>53</sup>  $\ell < a$ ).

In conclusion, the statistics of eigenstates in 3D samples, modeled by the Anderson Hamiltonian on the simple cubic lattice with  $N = 16^3$  sites, have been studied. The disorder is introduced either on the diagonal (potential energy) or in the hopping (off-diagonal) matrix elements. Also calculated are the average Inverse Participation Ratio of the eigenstates as well the conductance of different samples as a function of energy. This set of parameters allows us to compare the eigenstates in 3D

nanoscale mesoscopic conductors with different type of disorder, but characterized by similar values of conductance. Sample-specific details, which are not parameterized by the conductance alone, are found. This is in spite of the fact that dimensionality, shape of the sample, and conductance (i.e., the eigenvectors and eigenvalues of the classical diffusion operator) are expected to determine the finite-size (and non-universal) corrections to universal (sample-independent) predictions of Random Matrix Theory. The appearance of pre-localized states is clearly exhibited in the 3D samples at criticality and is directly related to the extensively studied multifractal structure of these wave functions. Nevertheless, even in the delocalized metallic ( $g \gg 1$ ) phase, where the correlation length<sup>6</sup>  $\xi_c$  expected from the sample conductance  $g(\xi_c) = \mathcal{O}(1)$  is microscopic ( $L < \xi_c$  would naturally account for the multifractal  $\equiv$ critical wave functions,<sup>6</sup> like in 2D), pre-localized states are found in the band center of the random hopping (“off-diagonal”) disordered systems.

Inspiring discussions with V. Z. Cerovski are acknowledged. Valuable suggestions and guidance have been provided by P. B. Allen. The important improvements of the initial cond-mat preprint are the result of correspondence with B. Shapiro and I. E. Smolyarenko. This work was supported in part by NSF grant no. DMR 9725037.

† Present address: Department of Physics, Georgetown University, Washington, DC 20057-0995.

---

<sup>1</sup> P. W. Anderson, Phys. Rev. **109**, 1492 (1958).

<sup>2</sup> B. Kramer and A. MacKinnon, Rep. Prog. Phys. **56**, 1469 (1993).

<sup>3</sup> P. A. Lee and T. V. Ramakrishnan, Rev. Mod. Phys. **57**, 287 (1985).

<sup>4</sup> E. Abrahams, P. W. Anderson, D. C. Licciardello, and T. V. Ramakrishnan, Phys. Rev. Lett. **42**, 673 (1979).

<sup>5</sup> *Mesoscopic Quantum Physics*, edited by E. Akkermans, J.-L. Pichard, and J. Zinn-Justin, Les Houches, Session LXI, 1994 (North-Holland, Amsterdam, 1995).

<sup>6</sup> M. Janssen, Phys. Rep. **295**, 1 (1998).

<sup>7</sup> B. L. Altshuler, V. E. Kravtsov, and I. V. Lerner, in *Mesoscopic phenomena in solids*, edited by B. L. Altshuler, P. A. Lee, and R. A. Webb (North-Holland, Amsterdam, 1991).

<sup>8</sup> B. Shapiro, Phil. Mag. B **56**, 1031 (1987).

<sup>9</sup> K. Müller, B. Mehlig, F. Milde, and M. Schreiber, Phys. Rev. Lett. **78**, 215 (1997).

<sup>10</sup> V. Uski, B. Mehlig, R. A. Römer, M. Schreiber, cond-mat/0005380.

<sup>11</sup> K. B. Efetov, *Supersymmetry in Disorder and Chaos* (Cambridge University Press, Cambridge, 1997).

<sup>12</sup> C. W. J. Beenakker, Rev. Mod. Phys. **69**, 731 (1997).

<sup>13</sup> *Chaos in Quantum Physics*, edited by M.-J. Jiaonni, A. Voros, and J. Zinn-Justin, Les-Houches, Session LII, 1989 (North-Holland, Amsterdam, 1991).

<sup>14</sup> E. Akkermans and G. Montambaux, Phys. Rev. Lett. **68**, 642 (1992).

<sup>15</sup> T. Ghur, A. Müller-Groeling, and H. A. Widenmüller, Phys. Rep. **299** 189 (1998).

<sup>16</sup> For a recent comprehensive review see: A. D. Mirlin, Phys. Rep. **326**, 259 (2000).

<sup>17</sup> B. A. Muzykantskii and D. E. Khmel'nitskii, Phys. Rev. B **51** 5480 (1995).

<sup>18</sup> J. A. Folk *et al.*, Phys. Rev. Lett. **76**, 1699 (1996); A. M. Chang *et al.*, Phys. Rev. Lett. **76**, 1695 (1996).

<sup>19</sup> P. Pradhan and S. Sridhar, Phys. Rev. Lett. **85**, 2360 (2000).

<sup>20</sup> Y. V. Fyodorov and A. D. Mirlin, Phys. Rev. B **51**, 13 403 (1995).

<sup>21</sup> V. I. Fal'ko and K. B. Efetov, Phys. Rev. B **52** 17 413 (1995).

<sup>22</sup> E. J. Heller, Phys. Rev. Lett. **53**, 1515 (1984).

<sup>23</sup> L. P. Gor'kov, A. I. Larkin, and D. E. Khmel'nitskii, Pis'ma Zh. Eksp. Teor. Fiz. **30**, 248 (1979) [JETP Lett. **30**, 228 (1979)].

<sup>24</sup> S. Chakravarty and A. Schmid, Phys. Rep. **140**, 195 (1986).

<sup>25</sup> Note that random Hamiltonians of real disordered solids are tied to the real-space representation (i.e., matrix elements in this representation are spatially dependent, and e.g., TBH (2) is a band diagonal matrix, while all elements of random matrices in standard RMT ensembles are non-zero and spatially independent). Therefore, they do not satisfy statistical assumptions of the standard RMT ensembles.<sup>26</sup> Nevertheless, the connection to RMT statistics is provided by Efetov's supersymmetric approach.<sup>11</sup>

<sup>26</sup> Y. V. Fyodorov, in Ref. 5.

<sup>27</sup> L. P. Gor'kov and G. M. Eliashberg, Zh. Eksp. Teor. Fiz. **48**, 1407 1965 [Sov. Phys. JETP **21** 1965].

<sup>28</sup> C. E. Porter and R. G. Thomas, Phys. Rev. **104**, 483 (1956).

<sup>29</sup> V. I. Fal'ko and K. B. Efetov, Phys. Rev. B **50**, R11 267 (1994).

<sup>30</sup> B. L. Altshuler and B. I. Shklovskii, Zh. Eksp. Teor. Fiz. **91**, 220 (1986) [Sov. Phys. JETP **64**, 127 (1986)]; A. V. Andreev and B. L. Altshuler, Phys. Rev. Lett **75**, 902 (1995).

<sup>31</sup> V. N. Prigodin and B. L. Altshuler, Phys. Rev. Lett. **80** 1944 (1998).

<sup>32</sup> B. I. Shklovskii, B. Shapiro, B. R. Sears, P. Lambrianides and H. B. Shore, Phys. Rev. B **47**, 11 487 (1993).

<sup>33</sup> F. Wegner, Z. Phys. B **36**, 209 (1980).

<sup>34</sup> A. D. Mirlin and F. Evers, Phys. Rev. B **62**, 7920 (2000).

<sup>35</sup> M. Inui, S. A. Trugman, and E. Abrahams, Phys. Rev. B **49**, 3190 (1994), and references therein.

<sup>36</sup> P. W. Brouwer, C. Mudry, B. D. Simons, and A. Altland, Phys. Rev. Lett. **81**, 862 (1998).

<sup>37</sup> V. Z. Cerovski, cond-mat/0008308.

<sup>38</sup> F. J. Dyson, Phys. Rev. **92**, 1331 (1953).

<sup>39</sup> P. W. Brouwer, C. Mudry, and A. Furusaki, cond-mat/9904201.

<sup>40</sup> P. Cain, R. A. Römer, and M. Schreiber, Ann. Phys. (Leipzig) **8**, 507 (1999).

<sup>41</sup> K. Slevin, T. Ohtsuki, and T. Kawarabayashi, Phys. Rev. Lett. **84** 3915 (2000).

<sup>42</sup> R. Landauer, Phil. Mag. **21**, 863 (1970); C. Caroli, R. Combescot, P. Nozieres, and D. Saint-James, J. Phys C **4**, 916 (1971); Y. Meir and N. S. Wingreen, Phys. Rev. Lett. **68**, 2512 (1992).

<sup>43</sup> S. Datta, *Electronic Transport in Mesoscopic Systems* (Cambridge University Press, Cambridge, 1995).

<sup>44</sup> B. K. Nikolić and P. B. Allen, J. Phys. Condens. Matter **12**, 9629 (2000).

<sup>45</sup> H. A. Weidenmüller, Physica A **167**, 28 (1990).

<sup>46</sup> D. Braun, E. Hofstetter, A. MacKinnon, and G. Montambaux, Phys. Rev. B **55**, (1997).

<sup>47</sup> P. Markoš, Phys. Rev. Lett. **83**, 588 (1999).

<sup>48</sup> M. J. Calderon, J. A. Vergés, and L. Brey, Phys. Rev. B **59**, 4170 (1999).

<sup>49</sup> I. E. Smolyarenko and B. L. Altshuler, Phys. Rev. B **55**, 10 451 (1997).

<sup>50</sup> The usage of the term pre-localized (or anomalously localized) in 3D systems is somewhat ambiguous, e.g., compare Refs. 6,16,21,49.

<sup>51</sup> A. Altland and B. D. Simons, J. Phys A **32**, L353 (1999).

<sup>52</sup> A. D. Mirlin and Y. V. Fyodorov, J. Phys. A **26**, L551 (1993).

<sup>53</sup> B. K. Nikolić and P. B. Allen, cond-mat/0005389 (to appear in Phys. Rev. B Rapid Communications).

<sup>54</sup> T. N. Todorov, Phys. Rev. B **54**, 5801 (1996).

<sup>55</sup> B. L. Altshuler and B. D. Simons, in Ref. 5.